Risky business? Behavioral and neural mechanisms underlying risky decision-making in adolescents

Blankenstein, N.E.

Chapter 4

Neural tracking of subjective value under risk and ambiguity in adolescence

This chapter is under review as: Blankenstein, N. E., & van Duijvenvoorde, A. C. K. Neural tracking of subjective value under risk and ambiguity in adolescence.

Abstract

Although many neuroimaging studies on adolescent risk taking focus on brain activation during outcome valuation, less attention is paid to the neural correlates of choice valuation. Subjective choice valuation may be particularly influenced by whether a choice presents risk (unknown outcomes with known probabilities) or ambiguity (unknown outcomes with unknown probabilities), which has rarely been studied in developmental samples. Therefore, we examined the neural tracking of subjective value during choice under risk and ambiguity in a large sample of adolescents (N = 188, 12-22 years). Specifically, we focused on whether risk and ambiguity were coded by activation in distinct or overlapping brain regions. A model-based approach to estimate individuals' risk and ambiguity attitude showed that there was prominent individual variation in individuals' aversion to risk and ambiguity. Furthermore, participants subjectively experienced the ambiguous options as riskier compared to the risky options. On the neural level we observed that subjective value tracking under risk was coded by activation in ventral striatum and superior parietal cortex. In contrast, subjective value tracking under ambiguity was coded by dorsolateral prefrontal cortex (PFC) and superior temporal gyrus activation. Finally, dorsomedial PFC activation reflected a common neural signal of subjective choice valuation, coding both risk and ambiguity. Together, this study indicates distinct and overlapping brain activation patterns for choice valuation under risk and ambiguity in an adolescent sample. Finally, we highlight the potential of combining behavioral modelling with fMRI for investigating choice valuation in adolescence, which may ultimately aid in understanding who takes risks and why.

Key words: adolescence, subjective value, risk, ambiguity, fMRI, parametric

Introduction

Adolescence encompasses the developmental phase from childhood to adulthood, and is often described as a period marked by increases in risk-taking tendencies such as reckless driving behavior and heightened levels of substance use (Crone & Dahl, 2012; Somerville, Jones, & Casey, 2010). To date, most research on adolescent risk taking has focused on relating reward processes under different conditions of risk, to task-based or real-life risk-taking behavior, and have observed meaningful relations. For instance, higher levels of real-life risk-taking have been associated with attenuated activation in lateral prefrontal regions during reward outcome processing, following decisions under risk (known probabilities) as well as ambiguity (unknown probabilities; Blankenstein, Schreuders, Peper, Crone, & van Duijvenvoorde, 2018). Surprisingly, fewer studies have focused on choice processes, and the development of choice valuation that may drive risk-taking behavior. In particular, classic economic theories posited that expected value, i.e., the product of the magnitude and the probability of the outcome, determines choice behavior, in which a higher objective value should be the more attractive choice. However, individuals' subjective evaluation of choice options rarely matches the objective expected value (Kahneman & Tversky, 1979). Therefore, subjective, rather than objective, choice valuation may be a more sensitive reflection of individual valuation processes (van den Bos, Bruckner, Nassar, Mata, & Eppinger, 2017). Moreover, subjective valuation of risk and ambiguity have been suggested to be sensitive to developmental change (Blankenstein, Crone, van den Bos, & van Duijvenvoorde, 2016; Tymula et al., 2012; van den Bos & Hertwig, 2017), but also shows large individual variation in adolescence (Blankenstein et al., 2016; Blankenstein et al., 2018). To date, few studies have explicitly focused on the behavioral and neural correlates of subjective, and expected, value tracking in adolescents, nor under conditions of risk and ambiguity. The current study therefore set out to investigate the behavioral and neural correlates of subjective value tracking under risk and ambiguity in a large sample of adolescents.

One common decision strategy suggested by influential behavioral economic theories such as prospect theory posits that when an individual is confronted with a decision between two alternatives, they first ascertain the subjective value of each available choice option, and then select the option with the highest subjective value (Kahneman & Tversky, 1979). A comprehensive meta-analysis of 206 studies examined the neural basis of subjective value in adults across a wide range of reward types (Bartra, McGuire, & Kable, 2013). This meta-analysis identified the anterior insula, dorsomedial prefrontal cortex (DMPFC), dorsal striatum, and

thalamus as key regions that have been found to code *both* positive and negative effects of subjective value on brain activation. That is, some studies have found activation increases in these regions with increasing subjective value, while others found activation increases in these regions with decreasing subjective value. This mixture of positive and negative effects was interpreted as a signal of salience or arousal (Bartra et al., 2013). Conversely, the ventral striatum (VS) and ventromedial prefrontal cortex (VMPFC) have been found to predominantly reflect positive effects of subjective value for different reward types (Bartra et al., 2013; Rangel & Clithero, 2014; Sescousse, Caldú, Segura, & Dreher, 2013).

Few studies have examined the neural signature of choice valuation in adolescents. Studies that focused on expected value coding during choice in children, adolescents, and adults (Barkley-Levenson & Galván, 2014; Van Duijvenvoorde et al., 2015), and showed that activation in VS, DMPFC, dorsolateral prefrontal cortex (DLPFC), and parts of the parietal cortex were positively related to increases in expected value. In addition, activation in VS was more pronounced with increasing expected value for adolescents compared with adults, highlighting that adolescents are more sensitive to these increases than adults, even when the adolescents were compared with adults who displayed similar gambling behavior (Barkley-Levenson & Galván, 2014). Importantly, these studies focused only on objective expected value scaling in adolescents. However, studies integrating the subjective evaluation of value are currently lacking and may be important because the expected value of a choice option may not exactly match an individual's subjective value of the choice at hand (van den Bos et al., 2017).

An important factor that contributes to individuals' (subjective) choice valuation is whether the choice alternatives reflect explicit risk or ambiguous risk. That is, in situations in which the decision outcomes are uncertain, explicit risk (henceforth referred to as risk) reflects decision environments in which the probabilities are known, whereas ambiguous risk (henceforth referred to as ambiguity) reflects decision environments in which the probabilities are unknown (Tversky & Kahneman, 1992). Not only are there considerable individual differences in the level of risk and ambiguity preferences (ranging from aversion to seeking), they may also vary across development, and are differentially related to overt risk-taking levels (Blankenstein et al., 2016; Tymula et al., 2012; van den Bos & Hertwig, 2017). On the neural level, deciding under conditions of risk and ambiguity have been found to be coded by different brain regions, particularly when considering individual differences in risk-taking levels under risk and ambiguity, in both adults and adolescents (Blankenstein, Peper, Crone, & Duijvenvoorde, 2017; Blankenstein et al., 2018). On the other hand, a key study comparing neural coding between risk and ambiguity in adults

showed that striatum, MPFC, PCC, and amygdala positively scaled with increases in subjective value under *both* risk and ambiguity. That is, in this study none of these brain regions conveyed unique information about subjective value under either risk or ambiguity. This suggests that at least in adults, subjective value tracking under risk and ambiguity is similarly represented in the brain, even though behavior under these conditions differs considerably (Levy, Snell, Nelson, Rustichini, & Glimcher, 2010). However, whether subjective value scaling under conditions of risk versus ambiguity differs or is similarly represented in adolescence, has yet to be examined.

Taken together, this follow-up study on Blankenstein et al. (2018) investigates subjective value tracking under risk and ambiguity, by combining an fMRI gambling task with separately estimated risk and ambiguity attitudes, in a large sample of adolescents (N = 188, 12-22 years). The goals of this study were threefold. First, we studied which regions code subjective value under risk and ambiguity, and investigated differences and similarities between these conditions. Second, we examined how these results compare to objective, rather than subjective, value coding. Finally, we explored whether there were age effects in subjective value coding. We hypothesized that activation in the VS, VMPFC, and parietal cortex in particular would increase with increasing subjective value (Barkley-Levenson & Galván, 2014; Van Duijvenvoorde et al., 2015). Given the mixed findings on DMPFC and insula, we expected that activation in DMPFC and insula could increase or decrease with increasing subjective value (Barkley-Levenson & Galván, 2014; Bartra et al., 2013). Specifically, to assess whether subjective value coding under risk and ambiguity relied on similar (Levy et al., 2010) or separate neural correlates in adolescence, we tested for unique activation patterns, as well as for overlap between conditions of risk and ambiguity. Although not necessarily within an adolescent age range, prior studies reported age differences in expected value tracking from adolescence into adulthood (Barkley-Levenson & Galván, 2014; Van Duijvenvoorde et al., 2015). Therefore, we explored linear and quadratic effects of age on the neural tracking of subjective value.

Methods

Participants

Two hundred and fourteen individuals (109 females, 105 males) between 12 and 22 years old participated in this study. Participants were part of a three-wave longitudinal study (Braintime; see for instance Peters & Crone, 2017, and Schreuders et al., 2018). Data of this sample has previously been reported in the cross-sectional study by Blankenstein et al. (2018). In this prior study, eighteen participants were

excluded because of psychiatric disorders, excessive head motion in the MRI scanner (> 3 mm), loss of data, and because of too few trials in which the gambling option was chosen in the fMRI task. For the goals of the current study we excluded ten additional participants because of violations of stochastic dominance in at least 50% of trials of the behavioral task (indicating a limited understanding of the task) and because of extreme outliers in risk attitude (i.e., > 3.5 *SD's* above the mean; in- or exclusion of these participants did not qualitatively affect our main behavioral or neural findings). The final sample therefore included 188 participants (100 female, 88 male, M_{Age} = 17.18, SD_{Age} = 2.59, range 12.02 – 22.02 years). An overview of the number of participants across age is provided in Figure S1A in the supplements. IQ was estimated in the first two waves, fell in the normal range, and did not correlate with age (see also Blankenstein et al., 2018; Peters & Crone, 2018; Schreuders et al., 2018).

The institutional review board of the University Medical Center approved this study. Written informed consent was given by adult participants, and by parents in the case of minors (minors provided written assent). All anatomical scans were cleared by a radiologist. Participants were screened for psychiatric or neurological disorders and MRI contra indications (none were observed).

Wheel of fortune task

fMRI task

Participants played a wheel-of-fortune task in the MRI scanner (see Figure 1; Blankenstein et al., 2017; Blankenstein et al., 2018). Here, participants were asked to make a series of decisions between a 'safe' wheel (presenting a consistent sure gain of €3) and a gambling wheel (presenting a chance of winning more money (€31-€34), but also a chance of winning nothing (€0)). The gambling wheel could either be risky (probabilities were known: 0.25, 0.50, or 0.75) or ambiguous (probabilities were hidden). After the decision, participants were presented with the outcome (gain or no gain). Behavioral results of the fMRI task are provided in the supplements (Figure S1B).

Ninety-two trials were presented: 46 ambiguous and 46 risky trials. Of the risky trials, 30 trials reflected a gamble with a 50% probability of winning, 8 trials reflected a gamble with a 75% probability of winning, and 8 trials reflected a gamble with a 25% probability of winning. The experiment was programmed such that these probabilities matched the actual probabilities of winning. Furthermore, one of the four possible amounts (€31, €32, €33, or €34) were randomly displayed (without replacement), on a trial-by-trial basis. Thus, although each participant was presented with the same distribution of probabilities, the amount varied per trial.

The task was presented in the scanner via E-prime (Psychology Software Tools).

Participants were presented with the pairs of wheels. Gamble and safe options were randomly displayed on the left or right side of the screen on a trial-by-trial basis, and the position of the blue and red parts of the risky wheels (left, right, bottom, and top of the wheel) were counterbalanced across trials. A gray square prompted the participants to give a response, which had to be given within a 3000 msec interval. A selection frame around the chosen wheel confirmed the response, and remained visible for the duration of the interval. The decision phase was separated from the outcome phase by a fixation cross of 2-4 seconds (jittered, with increments of 500 msec). Reward outcomes were presented for 1250 msec. The inter-trial-intervals and the optimal trial sequence were determined with OptSeq (Dale, 1999), with jittered intervals varying between 0 and 9350 msec. In addition, each trial was preceded by a 500 msec fixation cross, which was not part of the inter-trial-interval.

Behavioral task

Following the scan session, participants played a behavioral version of the wheel of fortune task (as validated previously, see Blankenstein et al., 2017; Blankenstein et al., 2016). This task includes more variation in probabilities (0.125, 0.25, 0.375, 0.50, 0.625, 0.75), amounts (€5, €8, €20, €50) and ambiguity level (0%, 25%, 50%,

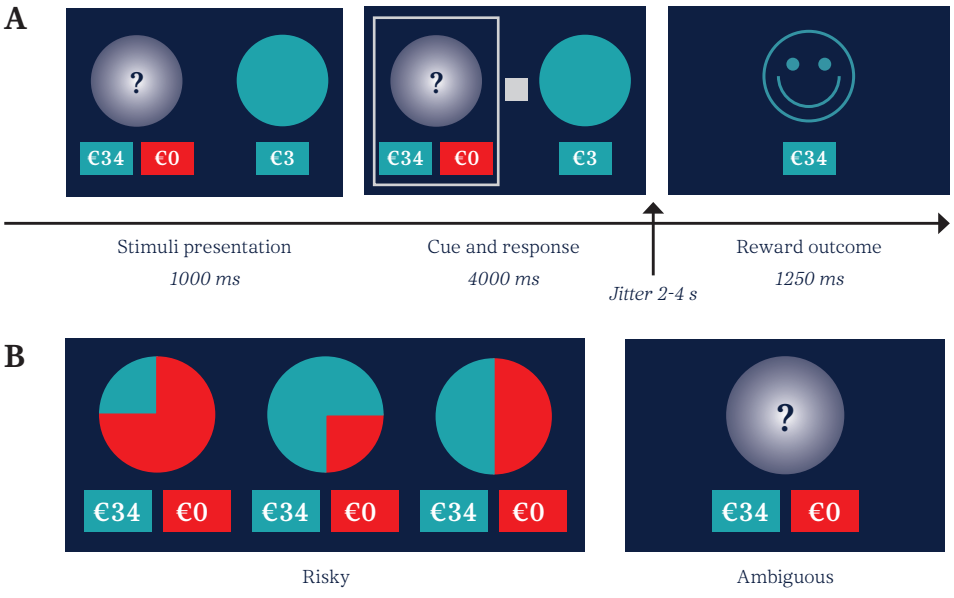

Figure 1. *Schematic representation of the fMRI task.* ***A.*** *Example of an ambiguous trial in which the outcome after choosing to gamble was gain.* ***B.*** *Risky and ambiguous stimuli.*

75%, 100%), allowing the model-based estimation of each individual's risk and ambiguity attitudes. No decision outcomes were provided in this task to ensure that the resulting risk and ambiguity attitudes could not be influenced by differences in the choice environment. The task included 24 unique risk trials (all probabilities combined with all amounts), and 16 unique risk trials (all ambiguity levels combined with all amounts). All trial types were presented twice, resulting in 80 trials used for the model-based estimations of risk and ambiguity attitudes.

Each trial started with a jittered fixation cross (500-1000 msec, with increments of 100 msec) followed by the wheels. A gray square in the center of the screen prompted the participants to respond (reaction time was self-paced), and a selection frame confirmed the participant's choice. The wheels (gamble, safe) were randomly displayed right and left on the screen, and the position of the blue and red portions of the risky wheels, and the position of the ambiguous lids (top or bottom) were counterbalanced across trials.

Risk and ambiguity attitude estimations

We estimated each participant's risk and ambiguity attitude from the behavioral task by modelling the expected utility (EU) of each choice option, using a power utility function with an additional term that takes into account ambiguity attitude (Blankenstein et al., 2016; Gilboa & Schmeidler, 1989; Levy et al., 2010; Tymula et al., 2012):

$$EU(x,p,A) = (p - \beta * \frac{A}{2}) * x^{\alpha} \qquad \textit{Equation 1.}$$

where x indicates the amount, p the probability, A the ambiguity level, α the risk attitude, and β the ambiguity attitude. A risk attitude of 1 indicates risk-neutrality, a risk attitude of < 1 indicates risk-aversion, and a risk attitude > 1 indicates risk-seeking. Relatedly, an ambiguity attitude of 0 indicates ambiguity-neutrality (meaning the participant is unaffected by the level of ambiguity), an ambiguity attitude > 0 indicates ambiguity-aversion (meaning the participants behaves as if the probability is less than the objective probability (50%), and an ambiguity attitude < 1 indicates ambiguity-seeking (meaning the participant behaves as if the probability is more than the objective probability).

For model fitting, the simplex algorithm of the general purpose optimization toolbox (optim) in R was used (R Core Team, 2015). To model trial by trial choices, a logistic choice rule was used to compute the probability of choosing to gamble (Pr(*ChoseGamble*) as a function of the difference in expected utility of the gamble (EU_{Gamble}) and the safe option (EU_{Safe}). Furthermore, the decisions of the participants

were modeled as susceptible to an error term (μ) to account for potential stochasticity in choice.

$$\Pr(ChoseGamble) = \frac{1}{1 + \exp(-(EU_{Gamble} - EU_{Safe}) / \mu)} \qquad \textit{Equation 2.}$$

This function was refitted with a grid search procedure to account for local minima in the estimated parameters. The resulting risk and ambiguity attitudes were used for behavioral analyses and to set up the parametric regressors for the whole-brain fMRI analyses (see 'General Linear Model'). In the supplementary materials we report the results of analyses on the raw choice behavior in the behavioral task (Figure S1C). In brief, these results show that participants were sensitive to the task parameters (amount, probability, ambiguity level), and thus that participants had a basic understanding of the behavioral task. Furthermore, on average, participants gambled an equal amount in the risky and ambiguous trials, but responded slower in the ambiguous than in the risky trials.

Exit questions subjective experience

To examine participants' subjective experience of the gambling wheels in the behavioral task, we presented participants with a number of exit questions following the behavioral task. Specifically, we presented participants with the different risky (0.125, 0.25, 0.375, 0.50, 0.625, 0.75 probabilities) and ambiguous (25%, 50%, 75%, 100%) wheels, without showing the amounts, and asked participants for each of these wheels how risky they found this wheel. Participants could indicate their perceived riskiness on a slider bar (0-100).

Procedure

The procedure was similar to Blankenstein et al. (2017; 2018). Participants were accustomed to the MRI environment using a mock scanner and received instructions on the wheel of fortune task in a quiet laboratory room. We explained participants that the ambiguous wheel could reflect a gamble of any of the risky probabilities (25%, 50%, 75%). Participants completed ten practice trials. In the scanner, participants responded to the task with their right hand using a button box, and head movements were restricted with foam padding. The fMRI task was followed by a high-definition structural scan.

After the MRI session, participants completed the behavioral version of the wheel of fortune task (see also Blankenstein et al., 2017), in which participants were given a hypothetical choice task and were instructed to choose which option they preferred. To explain the different ambiguity levels, we showed the different 'lids' that varied

in size and covered different proportions of the wheel, and showed the wheels that could lie underneath these lids. Participants practiced three trials beforehand.

Finally, participants completed the exit questions on their subjective experience of the wheels presented in the behavioral task, via Qualtrics (www.qualtrics.com). For other procedural details of the Braintime study that are not related to the current research goals, please see Blankenstein et al. (2018), Schreuders et al. (2018), and Peper & Crone (2018).

MRI data acquisition

We used a 3T Philips scanner (Philips Achieva TX) with a standard whole-head coil. Functional scans were acquired during two runs of 246 dynamics each, using T2* echo-planar imaging (EPI). Volumes covered the entire brain (repetition time (TR) = 2.2 s; echo time (TE) = 30 ms; sequential acquisition, 38 slices; voxel size 2.75 x 2.75 x 2.75 mm; field of view (FOV) = 220 x 220 x 114.68 mm). To allow for equilibration of T1 saturation effects we discarded the first two volumes. A high-resolution 3D T1 scan was obtained after the fMRI task for anatomical reference (TR = 9.76 msec, TE = 4.59 msec, 140 slices, voxel size = 0.875 mm, FOV = 224 × 177 × 168 mm).

MRI data analyses

Preprocessing

MRI preprocessing steps were identical to Blankenstein et al. (2018). Data was analyzed using SPM8 (Wellcome Department of Cognitive Neurology, London). Images were corrected for slice timing acquisition and rigid body motion. We spatially normalized functional volumes to T1 templates. Translational movement parameters never exceeded 3 mm (< 1 voxel) in any direction for any participant or scan. The normalization algorithm used a 12-parameter affine transform with a nonlinear transformation involving cosine basis function, and resampled the volumes to 3 mm^3 voxels. Templates were based on MNI305 stereotaxic space. The functional volumes were spatially smoothed using a 6 mm full width at half maximum (FWHM) isotropic Gaussian kernel.

General-Linear model

We used the general linear model (GLM) in SPM8 to perform statistical analyses on individual subjects' data. The fMRI time series were modeled as a series of two events: the decision phase and the outcome phase, convolved with a canonical hemodynamic response function (HRF). The onset of the decision phase was modeled with a duration of the participant's response (1000 msec + response time; see Figure 1), and the onset of the outcome phase (gain or no gain) was modeled with

zero duration. Events were modeled separately for risk and ambiguity. The GLM included the direct and parametrically modulated regressors of risk and ambiguity during the decision phase, and the direct regressors of gains and no gains during the outcome phase. In the current study, we were interested in the parametric tracking of subjective value under risk and ambiguity only, but in the supplements we show the main effects of choosing under risk and ambiguity (i.e., not parametrically modulated; Figure S2 A-B). Results of the main contrasts during the outcome phase are reported in Blankenstein et al. (2018).

Subjective value under risk and ambiguity were inferred by entering each individual's risk and ambiguity attitude, derived from the behavioral task, in Equation 1 for the trials in the fMRI task. That is, for each participant, we determined the subjective value of the wheel selected by the participant (gamble or safe) given the probability (0.25, 0.50, 0.75, or 1), amount (€3, €31, €32, €33, or €34), ambiguity level (0 or 1) of the selected wheel, and the participant's risk and ambiguity attitude derived from the behavioral task.

Trials on which participants did not respond were modeled separately as a regressor of no interest, and six motion parameters were included as nuisance regressors. The least-squares parameter estimates of the height of the best-fitting canonical HRF for each condition separately were used in pairwise contrasts. These pairwise comparisons resulted in individual-specific contrast images, which we used for the higher-level group analyses. All higher-level group analyses were conducted with Family Wise Error (FWE) cluster correction ($p < .05$, using a primary voxel-wise threshold of $p < .001$, uncorrected; Blankenstein et al., 2017; Woo, Krishnan, & Wager, 2014). We used the MarsBaR toolbox (Brett, Anton, Valabregue, & Poline, 2002; http://marsbar.sourceforge.net) to visualize patterns of activation in clusters identified in the whole-brain results. Coordinates of local maxima are reported in MNI space.

Results

Behavioral results

Risk and ambiguity attitude

First, we formally investigated the model-based estimations of risk and ambiguity attitude. To ease interpretation for these behavioral analyses, we recoded ambiguity attitude such that higher values indicate a relatively more seeking attitude. Figure 2A depicts box plots of risk and ambiguity attitude, with violin plots superimposed, which show the full distribution of the data. On average, participants were generally risk and ambiguity averse ($M_{risk} = .60$, $M_{ambig} = -.25$), although there were considerable

individual differences in these attitudes (SD_{risk} = .26, $range_{risk}$ =.11-1.52, SD_{ambig} = .36, $range_{ambig}$ = -1.00 – 1.00). Furthermore, participants did not differ in their degree of aversion to risk and ambiguity (p = .62, as indicated by a paired-samples t-test on z-transformed risk and ambiguity attitudes). Next, we tested for linear, quadratic, and cubic effects of age on risk and ambiguity attitudes using regression analyses. For risk attitude we observed a positive linear effect of age (R^2 = .02 , F(1, 186) = 4.29, b = .015, SE = .007, p = .04), indicating that risk-seekingness increased slightly across adolescence, while no effects of age were observed for ambiguity attitude (all *p's* > .1). Finally, a partial correlation showed that risk and ambiguity attitude, controlling for age, were not significantly correlated (*partial r* = -.083, p = .26).

Subjective experience behavioral task

To test the robustness of the behavioral estimates of risk and ambiguity attitudes, we examined participants' responses on the exit questions on perceived riskiness for each of the wheels in the behavioral task. First, a repeated measures ANOVA on the risky wheels with age linear and quadratic as covariates indeed showed that participants subjectively experienced the risky wheels as less risky with increasing gain probability (Figure 2B (left) main effect probability F(5, 920) = 154.99, p < .001, η_p^2 = .457; no effects of age (all p's > .25)). A similar finding was observed for the ambiguous wheels, in which participants subjectively experienced the ambiguous wheels as more risky with increasing ambiguity level (Figure 2B (right); main effect ambiguity level: F(3, 552) = 118.73, p < .001, η_p^2 = .392; no effects of age (all p's > .14)). On average, participants perceived the ambiguous wheels as riskier than the risky wheels (M_{ambig} = 62.75, SE_{ambig} = 1.22, M_{risk} = 52.52, SE_{risk} = .61, F(1, 184) = 54.50, p < .001, η_p^2 = .244, no effects of age (all p's > .16)).

Next we tested whether participants' average subjective experience was correlated with the behavioral estimations of risk and ambiguity attitude, while controlling for age. These partial correlations showed that risk attitude was negatively correlated with perceived riskiness of the risky wheels (*partial r* = -.21, p = .004, Figure 2C (left)), as well as of the ambiguous wheels (*partial r* = -.20 , p =.007, not depicted in a figure). Thus, a more risk-seeking attitude was correlated with perceiving these wheels as less risky. Finally, ambiguity attitude was correlated with the perceived riskiness of the ambiguous wheels (*partial r* = -.15, p = .043; Figure 2C (right)), such that a more seeking attitude was correlated with perceiving these wheels as less risky. This relation between ambiguity attitude and perceived riskiness of the risky wheels was not observed (*partial r* = .011, p = .88). Together, these findings show that the behavioral estimations of risk and ambiguity attitude also reflect participants' self-reported subjective experience of the gambles in the behavioral task

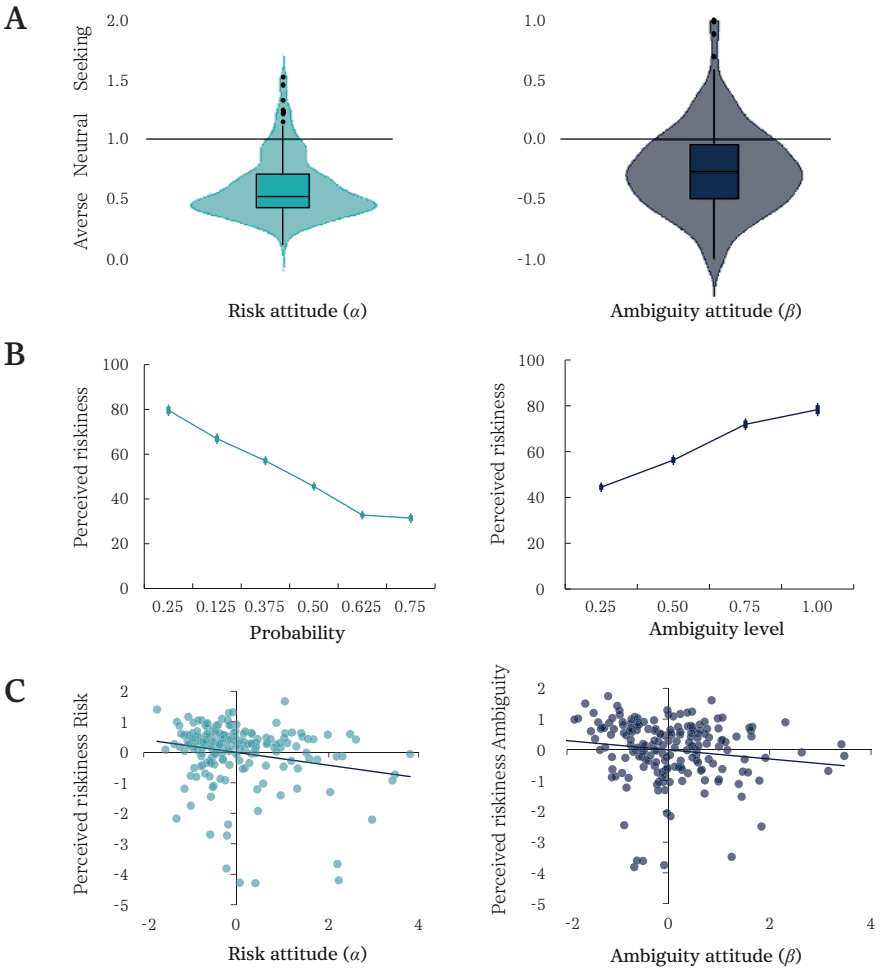

Figure 2. A. *Violin- and box-plots for risk attitude (left) and ambiguity attitude (right). The violin plots show the full distribution of the data. For risk attitude, 0 indicates risk aversion, 1 indicates risk neutrality, and 2 indicates risk seeking. For ambiguity attitude, -1 indicates ambiguity aversion, 0 indicates ambiguity neutrality, and 1 indicates ambiguity seeking. For both measures, participants were generally averse, although there were considerable individual differences.* ***B.*** *Average perceived riskiness for each of the risky wheels (left) and ambiguous wheels (right) presented in the behavioral task, controlled for age. Bars indicate standard errors.* ***C****. Partial correlations of risk attitude and the mean perceived riskiness of the risky wheels (left), and partial correlation of ambiguity attitude and the mean perceived riskiness of the ambiguous wheels (right), controlled for age. Risk attitude correlated with the perceived riskiness of both conditions, while ambiguity attitude only correlated with the perceived riskiness of ambiguity.*

fMRI results

Subjective valuation of risk and ambiguity

First, we examined the neural patterns of subjective value coding for risk and for ambiguity. To this end, we ran a whole-brain repeated measures ANOVA with condition (risk and ambiguity as parametric regressors) as within factor, and inspected the positive and negative *t*-contrasts for risk and ambiguity. For risk, we observed positive patterns of activation in bilateral VS, bilateral superior parietal cortex (SPL), postcentral gyrus, mid-cingulate cortex, and supplementary motor area, indicating that with increasing subjective value, activation in these regions increased. In addition, activation in DMPFC and right inferior parietal lobe (IPL) increased with decreasing subjective value (Figure 3A; Table 1).

For ambiguity, we observed subjective value coding also in DMPFC, but in addition in bilateral DLPFC, right superior temporal gyrus (STG), and bilateral inferior parietal lobe (IPL) (see Figure 3B, Table 1). In these regions decreasing subjective value was related to increasing neural activation. No positive activation patterns for ambiguity were observed.

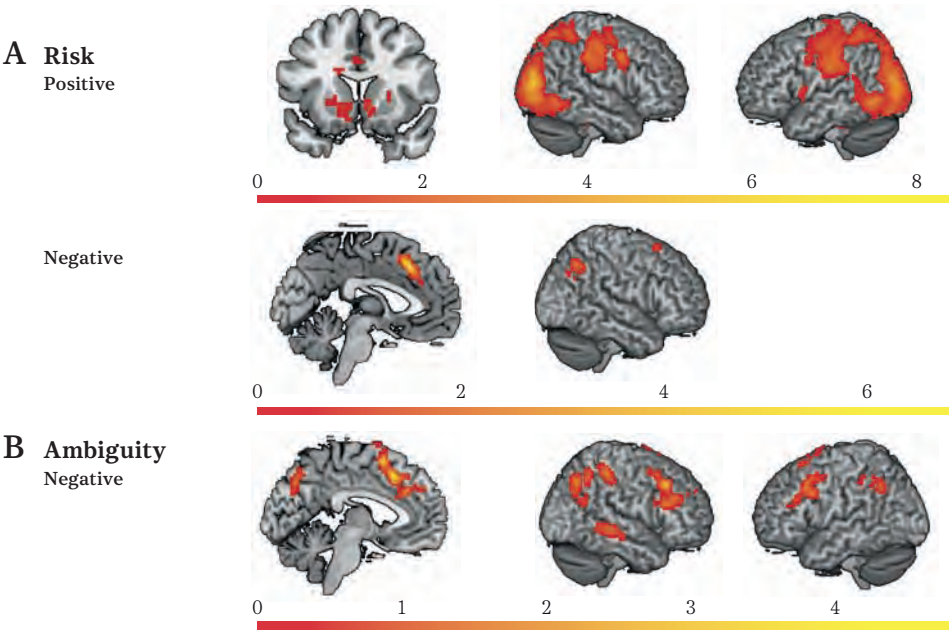

Figure 3. *Results of the whole-brain ANOVA, showing the unmasked T-contrasts for* ***A.*** *Risk positive (upper panel; y = 14; L; R); Risk negative (lower panel; x = -4; R)* ***B.*** *Ambiguity negative (x = -4; R; L). Results were FWE cluster-corrected (p < .05).*

Table 1. Results of unmasked *t*-contrasts for risk and ambiguity for subjective value.

Anatomical region	+/-	MNI coordinates x	y	x	T	*k*	*p*
Risk							
R middle occipital gyrus, including bilat. superior parietal lobe	+	30	-85	16	8,36	9610	< .001
R calcarine gyrus	+	15	-91	4	7,83		
R fusiform gyrus	+	30	-82	-8	7,68		
L insula lobe	+	-33	-4	16	5,18	1028	< .001
L putamen, including R and L caudate nucleus, L inferior frontal gyrus, L thalamus	+	-30	-10	-2	4,94		
R thalamus	+	21	-28	-2	5,05	299	< .001
R putamen, including R insula lobe	+	27	-10	7	4,92		
R middle cingulate cortex, including L middle cingulate cortex	+	12	5	43	4,17	269	< .001
R supplementary motor area	+	9	-1	58	4,08		
L supplementary motor area	+	-6	-1	52	3,54		
L superior medial gyrus	-	-6	23	40	6,86	324	< .001
R middle cingulate cortex	-	9	26	34	5,40		
R supplementary motor area, including R anterior cingulate cortex, R superior frontal gyrus	-	15	20	64	4,18		
Ambiguity							
R middle frontal gyrus	-	42	26	43	4,865	346	< .001
R inferior frontal gyrus	-	54	26	25	4,277		
R inferior frontal gyrus	-	42	32	28	4,102		
L supplementary motor area	-	-3	20	46	4,656	617	< .001
L supplementary motor area, including R supplementary motor area	-	-3	11	58	4,484		

Table 1. Continued

Anatomical region	+/-	MNI coordinates x	y	x	T	*k*	*p*
R anterior cingulate cortex, including L superior medial gyrus, L and R superior frontal gyrus, L anterior cingulate cortex	-	12	26	25	4,388		
R inferior parietal lobe	-	54	-37	55	4,48	394	< .001
R angular gyrus	-	36	-67	43	4,437		
R inferior parietal lobe	-	48	-55	52	4,12		
R middle temporal gyrus	-	66	-31	-2	4,247	146	.001
R middle temporal gyrus	-	63	-43	1	3,808		
L inferior frontal gyrus	-	-51	14	34	4,211	220	< .001
L middle frontal gyrus	-	-42	20	40	4,184		
L middle frontal gyrus	-	-42	14	49	3,949		
R precuneus	-	6	-67	40	3,959	156	.005
L precuneus, including L cuneus	-	-3	-73	37	3,844		
R cuneus, including L precuneus	-	9	-79	28	3,2		
L inferior parietal lobe	-	-48	-58	43	3,924	133	.011
L inferior parietal lobe	-	-45	-37	40	3,637		
L inferior parietal lobe, including L angular gyrus	-	-48	-40	52	3,387		

Note: L = left; R = right. Anatomical labels are based on the Automated Anatomical Labeling (AAL) atlas. Results were FWE cluster-corrected (p < .05).

Overlap risk and ambiguity

To formally test the overlap in the patterns of activation in risk and in ambiguity, we ran a conjunction analysis on the negative *t*-contrasts of risk and ambiguity from the whole-brain ANOVA (no positive activation patterns were observed for ambiguity, see above). To this end we used the 'Logical AND' technique, which requires that the contrasts included in the conjunction are individually significant (Nichols, Brett, Andersson, Wager, & Poline, 2005). The conjunction showed significant overlap in the DMPFC for the negative effects of risk and ambiguity (Figure 4A, Table 2), indicating that with decreasing subjective value, activation in this region increased, regardless of condition.

Unique effects of risk and ambiguity

Next, we investigated *unique* patterns of subjective value under risk and under ambiguity. That is, we tested for effects of risk restricted towards the voxels that were not activated under ambiguity (i.e., using exclusive masks), and vice versa. For risk, we observed unique patterns of positive activation in bilateral VS and bilateral SPL, and postcentral gyrus (Figure 4B, Table 2), indicating that with increasing subjective value under risk, activation in these regions increased. No unique patterns of negative activation were observed. For ambiguity, unique negative activation was found in bilateral DLPFC, right STG, and in right IPL (Figure 4C, Table 2), indicating that with decreasing subjective value under ambiguity, activation in these regions increased.

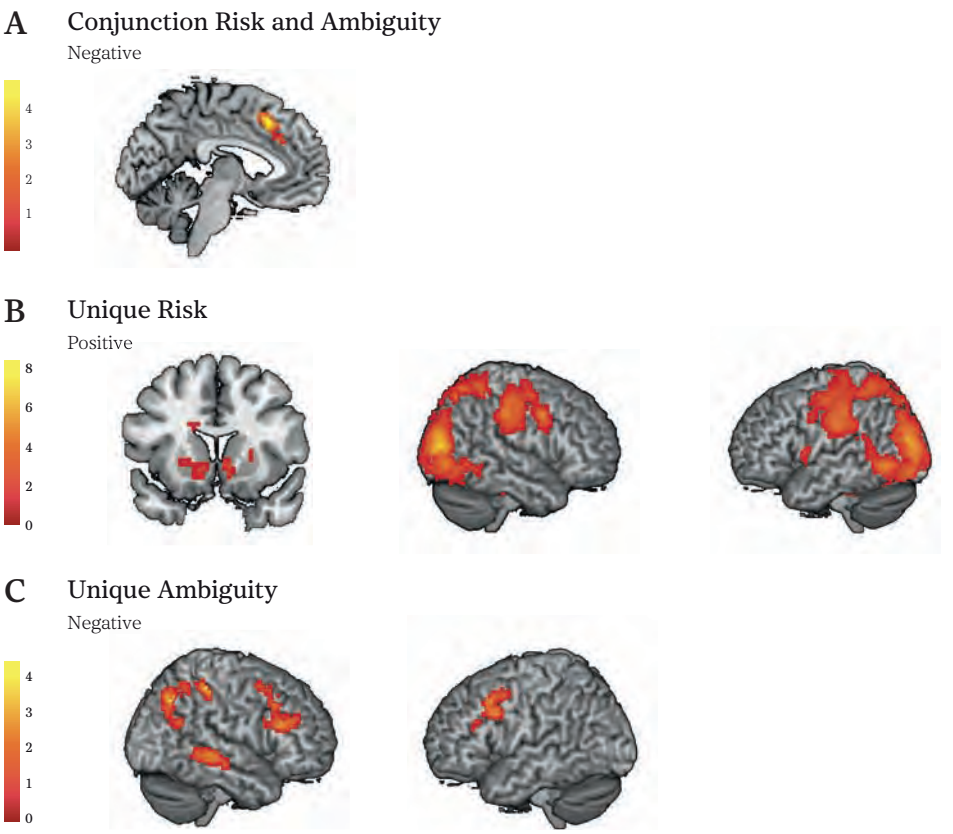

Figure 4. *Results of the whole-brain ANOVA, showing* ***A****. the conjunction between the negative effects of risk and ambiguity (x = -4)* ***B.*** *Risk positive, masked by Ambiguity (y = 14; L; R) and* ***C.*** *Ambiguity negative, masked by Risk (x = -4; R; L). Results were FWE cluster-corrected (p < .05).*

Table 2. Results of the whole-brain repeated measures ANOVA for subjective value.

		MNI coordinates					
Anatomical region	+/-	x	y	x	T	*k*	*p*
Conjunction risk and ambiguity							
L supplementary motor area	-	-3	20	46	4,66	168	.004
R anterior cingulate cortex	-	9	29	28	3,86		
L anterior cingulate cortex, including R middle cingulate cortex	-	-6	32	28	3,83		
Unique effect of risk							
R middle occipital gyrus, including bilat. superior parietal lobe	+	30	-85	16	8,36	7327	< .001
R calcarine gyrus	+	15	-91	4	7,83		
R fusiform gyrus	+	30	-82	-8	7,68		
R precentral gyrus	+	60	5	40	6,57	683	< .001
R postcentral gyrus, including R supramarginal gyrus	+	60	-19	52	6,18		
L insula lobe	+	-33	-4	16	5,18	995	< .001
L putamen, including R/L caudate nucleus, L thalamus, L inferior frontal gyrus	+	-30	-10	-2	4,94		
R thalamus	+	21	-28	-2	5,05	296	< .001
R putamen, including R insula lobe	+	27	-10	7	4,92		
Unique effect of ambiguity							
R inferior parietal lobe	-	54	-37	55	4,48	229	< .001
R angular gyrus	-	36	-67	43	4,44		
R angular gyrus	-	57	-58	25	3,81		
R inferior frontal gyrus (p. triangularis)	-	54	26	25	4,28	228	< .001
R middle frontal gyrus	-	42	20	40	4,10		
R inferior frontal gyrus (p. triangularis)	-	45	29	25	4,01		
R middle temporal gyrus	-	66	-31	-2	4,25	145	.007
L inferior frontal gyrus (p. opercularis)	-	-51	14	34	4,21	136	.01
L middle frontal gyrus	-	-42	17	43	4,06		
L inferior frontal gyrus (p. triangularis)	-	-54	29	28	3,50		
R precuneus	-	3	-67	37	3,64	149	.007
L precuneus	-	-3	-73	31	3,55		
R cuneus	-	9	-79	28	3,20		

Note: L = left; R = right. Anatomical labels are based on the Automated Anatomical Labeling (AAL) atlas. Results were FWE cluster-corrected (p < .05).

Expected versus subjective valuation of risk and ambiguity

Furthermore, we tested whether results from the conjunction, and the unique effects of risk and ambiguity, were also present in a model testing for expected value increases (i.e., probability * amount, not weighted by individuals' risk and ambiguity attitude). These results are reported in the supplementary materials (Figure S2 C-D; Table S1). In short, the conjunction observed in the model for subjective value was not present in the model for expected value. Furthermore, although results for risk were highly similar between models, results for ambiguity were less pronounced (i.e., activation in left DLPFC was no longer observed).

Effects of age

Finally, when including age (linear and quadratic) as a covariate on the *t*-contrasts of subjective, and expected, value under risk and ambiguity, we observed that these results remained the same, nor did we find any significant effects of age. This indicates that the parametric tracking of subjective and expected value under risk and ambiguity was independent of age in this adolescent sample.

Discussion

This study investigated the neural tracking of subjective value under risk and ambiguity in adolescence, by combining neural activation during an fMRI gambling task with separately estimated risk and ambiguity attitudes. We found pronounced differences in subjective value under risk (bilateral VS, SPL) and ambiguity (bilateral DLPFC, right STG), as well as overlapping activation between risk and ambiguity (DMPFC). These results were less pronounced when examining expected, rather than subjective, value, and were independent of age. Finally, behavioral risk and ambiguity attitudes showed limited developmental, but considerable individual indifferences, and echoed participants' self-reported perceived riskiness of the risky and ambiguous options. The following sections discuss these main findings in further detail.

Neural tracking of subjective value under risk and ambiguity

On the neural level, we observed that subjective value increases under risk were positively associated with increased activation in bilateral VS and SPL. Particularly the VS activation coincides with prior adult research on subjective value coding in general (Bartra et al., 2013), and has been suggested to predict risk-seeking choices (Engelmann & Tamir, 2009; Kuhnen & Knutson, 2005; Tobler, O'Doherty, Dolan, & Schultz, 2007). Interestingly, in a previous study we observed that greater

risk-seeking attitudes were associated with greater activation in neighboring, valuation, regions (medial and lateral orbitofrontal cortex) during risky gambles (in a separate sample of young adults (18-30 years) using the same experimental paradigms; Blankenstein et al., 2017). The current study extends this earlier work by using a parametric design in which subjective expected value was calculated on a trial-by-trial basis, indicating that neural coding of subjective valuation of risk is present in a similar set of regions in adolescence. Finally, the activation observed in parietal cortex fits well with prior adult research on assessing probabilities (Huettel, Song, & McCarthy, 2005) as well as with risk preference (both functionally (Huettel, Stowe, Gordon, Warner, & Platt, 2006) and structurally (Gilaie-Dotan et al., 2014)).

With respect to ambiguity, we observed that increased activation in superior temporal gyrus and bilateral DLPFC coincided with decreasing subjective value. In a separate sample of young adults (18-30 years) we observed that greater ambiguity-seeking attitudes were also associated with heightened superior temporal gyrus activation in a highly overlapping region (MNI coordinates: 63 -22 -5; Blankenstein et al., 2017). Thus, the superior temporal gyrus may be presented as a candidate region sensitive to individual differences in ambiguity valuation, although future studies may further investigate its specific direction of activation (increasing or decreasing with greater subjective valuation of ambiguity). Second, DLPFC activation has been suggested to foster exploration tendencies, and thus relates to more ambiguity-seeking attitudes (Huettel et al., 2006). Conversely, the DLPFC has also been associated with heightened cognitive control, and a reduced appetite for risk taking in tasks in which ambiguity can be reduced over time by experience (Fecteau et al., 2007; Knoch et al., 2006). The observation in the current study of heightened DLPFC activation with decreasing subjective valuation is in line with this latter interpretation (i.e., a reduced appetite for risk-taking). Together, the STG and DLPFC appear to play a key role in tracking individual differences in subjective valuation under ambiguity in adolescents.

Furthermore, we observed that activation in DMPFC coded both subjective value decreases under risk, as well as under ambiguity. The DMPFC (also commonly referred to dorsal anterior cingulate cortex) has been implicated in a majority of functions relation to motivation and cognitive control, and shifting decision strategies (Venkatraman, Payne, Bettman, Luce, & Huettel, 2009). The meta-analysis by Bartra et al. (2013) suggests that this region, which has been observed for both positive and negative effects of subjective value, plays a role in detecting arousal or saliency. In a similar vein, the Expected Value of Control theory (Shenhav, Botvinick, & Cohen, 2013) posits that activation in this region reflects general changes in task incentives or task difficulty. Suggestively, the negative coding of subjective value in the DMPFC

may be reflective of such changes in task incentives and task saliency, given that this region coded subjective value in both decision contexts, and thus did not differentiate between risk and ambiguity.

Subjective versus expected value coding under risk and ambiguity

In addition to testing subjective value under risk and ambiguity, we explored whether similar findings were observed in a model testing for objective expected value coding under risk and ambiguity (i.e., probability * amount, not weighted by individuals' risk and ambiguity attitude). Overall, we found similar, but less pronounced, results in this model (reported in the supplements). Specifically, similar to the model with subjective value, we found heightened activation in bilateral VS and SPL for increasing expected value under risk, but only right DLPFC and right IPL with decreasing expected value under ambiguity. Furthermore, we did not observe the common neural coding in DMPFC under risk and ambiguity in the model of expected value. On the one hand, these less pronounced findings may result from the fact that there was relatively little variation in the task parameters. That is, a limitation of the current fMRI task is that it includes no variation in ambiguity level, small variations in amounts, and only larger variations in probability level. Thus, not weighing expected value with individuals' risk and ambiguity attitude may have resulted in less variation in task parameters, and thus to fewer neural changes that could be detected. On the other hand, these findings may suggest that making use of subjective, rather than expected, valuation, is more meaningful when studying the neural underpinnings of (adolescent) choice valuation (Glimcher & Rustichini, 2004; van den Bos et al., 2017), and highlights the potential of this particular method. Nevertheless, future studies should replicate our findings, preferably by using a more elaborate task design.

Effects of age and individual differences in subjective valuation of risk and ambiguity

To assess individuals' preference towards risk and ambiguity, we made use of a behavioral task and a model-based approach. Concurring with previous findings, we observed that participants were generally risk- and ambiguity-averse, and responded slower in ambiguity compared with risk (Blankenstein et al., 2017). Furthermore, participants subjectively experienced the ambiguous wheels in the task as more risky, compared with the risky wheels. Moreover, we showed that behavioral risk aversion was associated with perceiving the risky and ambiguous wheels in the task as more risky, and ambiguity aversion with perceiving the ambiguous wheels as more risky. This latter finding in particular suggest that these model-based measures not only reflect behavioral tendencies under risk and ambiguity, but also reflect the

subjective experience of gambling behavior. In sum, these data suggest meaningful differences between individuals in subjective evaluation of risk under known (risk) and unknown (ambiguity) contexts. This inter-individual variability set the stage for testing our hypotheses on the neural tracking of subjective valuation under risk and ambiguity.

Behaviorally, we observed that risk-seeking slightly increased across adolescence, whereas no developmental change was observed for ambiguity attitudes. Previous findings observed heightened ambiguity tolerance in adolescents compared with adults (Blankenstein et al., 2016; Tymula et al., 2012) and for adolescents compared to children and adults (although in a loss frame only; van den Bos & Hertwig, 2017). Furthermore, risk attitudes have been found to either show no developmental trend (Blankenstein et al., 2016), show a quadratic peak in risk seeking in mid adolescents (van den Bos & Hertwig, 2017) or heightened risk aversion in adolescents compared with adults (Tymula et al., 2012). These previous studies included age ranges well into adulthood, or started in early childhood (Tymula et al.: 12-17 years and 30-50 years; van den Bos et al.: 8-22 years; Blankenstein et al.: 10-25 years). Together, the current findings indicate that a developmental window across adolescence and into young adulthood is suitable to test individual variation, but less meaningful to detect developmental change. An interesting next step would be to include young children (<8 years) and older adults (>25 years), to establish developmental differences in ambiguity and risk attitudes.

Finally, similar to the behavioral results, we did not observe any age effects (linear, nor quadratic) on neural patterns of activation. Prior studies have observed age differences in the neural tracking of expected value, specifically in VS (more pronounced in adolescents (13-17 years) compared with adults (25-30 years; Barkley-Levenson & Galván, 2014), and in VMPFC and parietal cortex (linear increases from childhood (8-11 years) to adolescence (16-19 years) to adulthood (25-34 years; Van Duijvenvoorde et al., 2015). However, in our previous study including the same participants, few age effects were observed on risk and ambiguity processing during gambling (Blankenstein et al., 2018). Furthermore, the fact that minimal age effects were observed behaviourally in the current study may further explain the absence of age effects on the neural coding of subjective and expected value. Again, including young children and older adults may prove valuable for future studies.

Conclusion

In this study, we aimed to extend previous research by explicitly investigating subjective value tracking under risk and ambiguity in a large sample of adolescents. Our findings suggest that the neural coding of subjective value under risk and ambiguity is reflected in both distinct and similar patterns of brain activation in adolescents. Moreover, these findings seem to suggest it is valuable to include subjective, rather than objective, measures of choice valuation in neuroimaging studies on adolescent risk taking. Indeed, behavioral estimations of risk and ambiguity preference showed considerable individual variation, which were reflected in individuals' self-reported perceived riskiness of the risky and ambiguous choice options. Furthermore, the limited age effects observed in the current study highlight the need for studying a wider age range to unravel these developmental differences with more certainty. Together, these findings help to gain insights into subjective valuation in adolescents, and suggest adolescence is an important developmental window in which differences between risky and ambiguous subjective value tracking may be more prominent than in adult samples. Finally, this study highlights the potential of combining model-based behavioral analyses with fMRI, which may ultimately aid in understanding who takes risks and why.

Supplementary Materials

Choice behavior fMRI task

In the fMRI task, participants gambled a considerable proportion of times in the risky and ambiguous condition, although these did not differ significantly (M_{risk} = .74, SE_{risk} = .015, M_{ambig} = .76, SE_{ambig} = .018, p = .13, no effects of age (linear or quadratic, all p's > .17)). Furthermore, there were considerable individual differences in gambling behavior (see Figure S1B). Finally, a repeated measures ANOVA with age (linear and quadratic) as a covariate showed that participants responded significantly slower in the ambiguous trials compared with the risky trials (M_{ambig} = 641.59 msec, SE_{ambig} = 14.26; M_{risk} = 597.06 msec, SE_{risk} = 12.89; $F(1, 185) = 8.79$, p = .003, η_p^2 = .045, no effects of age (linear or quadratic, all p's > .06)).

Choice behavior behavioral task

To investigate whether participants had a basic sensitivity to the parameters (amount, probability, ambiguity level) of the task outside the scanner, we examined raw choice behavior. Repeated measures ANOVAs with age group (12-16 years and 17-22 years, in line with Blankenstein et al., 2016) as a between-subjects factor showed that gambling behavior increased with increasing probability and amount, and decreased with increasing ambiguity level (see Figure S1C; main effect probability: $F(5, 930) = 570.91$, $p < .001$, η_p^2 = .754; age group * probability interaction effect: p = .498; main effect amount: $F(3, 558) = 915.59$, p = .83, η_p^2 = .831, age group * amount interaction effect: $F(3, 558) = 6.65$, $p < .001$, η_p^2 = .034; main effect ambiguity level: $F(3, 558) = 48.54$, $p < .001$, η_p^2 = .207, age group * ambiguity level interaction: p = .637). Thus, participants were sensitive to these parameters, indicating a general understanding of the task. Finally, paired-samples t-tests showed that on average, participants gambled an equal amount in the risky and ambiguous trials (p = .375, M_{risk} = .35, SE_{risk} = .007, M_{ambig} = .36, SE_{ambig} = .01), but that participants responded significantly slower in the ambiguous than in the risky trials ($t(187) = 3.462$, p = .001, M_{risk} = 470.75, SE_{risk} = 18.15, M_{ambig} = 495.11, SE_{ambig} = 18.96).

fMRI results for expected value

We tested whether the unique effects of risk and ambiguity, and the conjunction, were also present in a model testing for effects of objective expected value (i.e., product of probability and amount, not weighted by individuals' risk and ambiguity attitude). To this end we again ran a whole-brain repeated measures ANOVA with condition (risk and ambiguity as parametric regressors) as within factor, and we tested for effects of risk restricted towards the voxels that were not activated under ambiguity (i.e., using

exclusive masks), and vice versa. First, the positive effect of risk was highly similar in the expected value model, compared with the subjective value model, with activation in bilateral VS, SMA, and SPL (Table S1, Figure S2C). For ambiguity on the other hand, activation was less pronounced in right DLPFC and right IPL, and absent in left DLPFC (Table S1; Figure S2D). Moreover, in a conjunction analysis we observed that the activation in DMPFC observed for the negative effects of risk and ambiguity in subjective value, was not present in the model with expected value. Finally, as in the model with subjective value, all of these findings were independent of age.

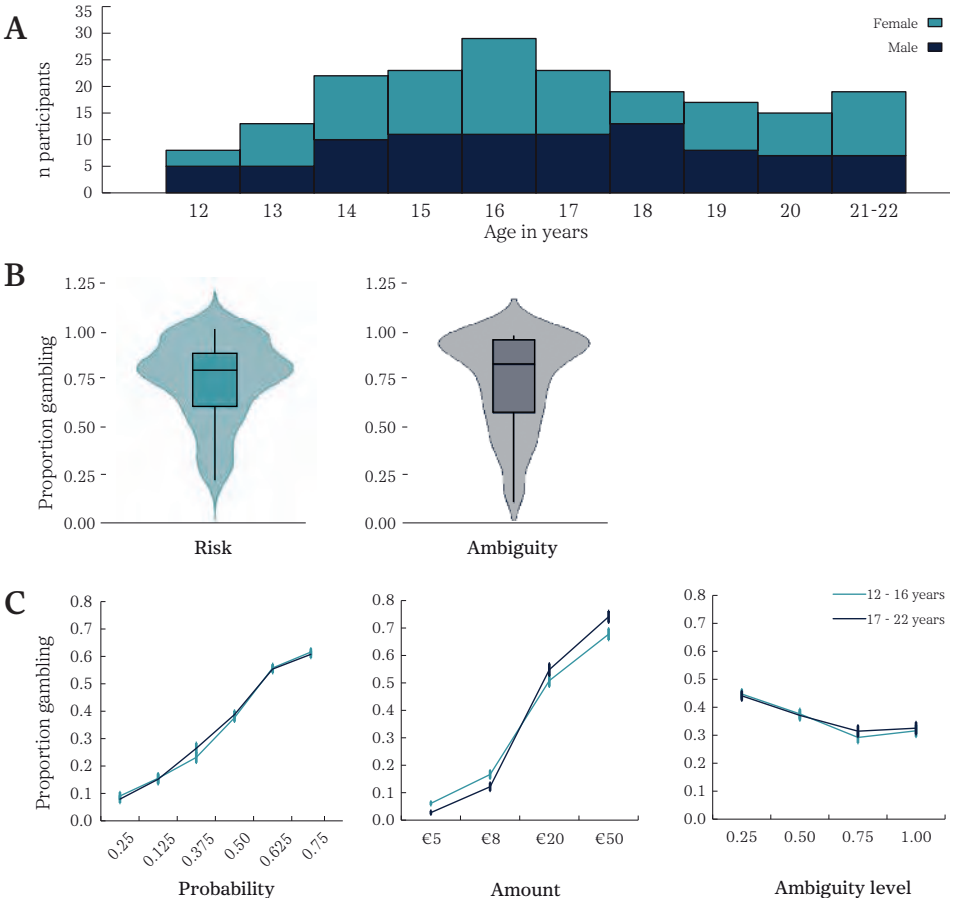

Figure S1. A. *Participant distribution across age.* ***B.*** *Violin- and box-plots of gambling under Risk (left) and Ambiguity (right).* ***C.*** *Proportion gambling for probability (left), amount (middle), and ambiguity level (right) per age group.*

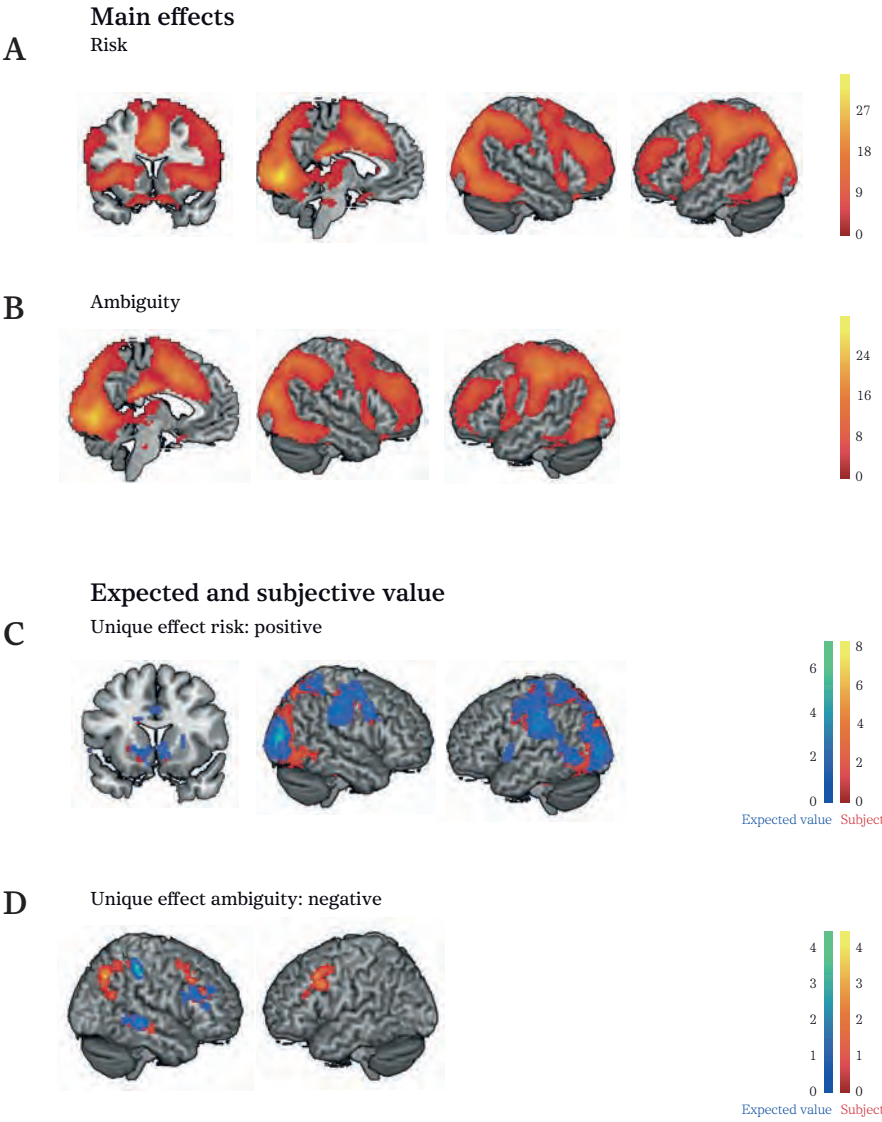

Figure S2. Upper panel: *Activation in the fMRI task during the decision-making phase (not parametrically modulated).* ***A.*** *Activation during risky decisions versus fixation (y = 14; x = -4; L; R).* ***B.*** *Activation during ambiguous decisions versus fixation (x = -4; L; R). Results were FWE voxel-corrected (p < .001).* ***Lower panel:*** *Expected and subjective value. Results of the unique effects of* ***C.*** *risk positive (y = 14; L; R). and* ***D.*** *ambiguity negative (R; L). Activation in blue represents activation for expected value, activation in red represents activation for subjective value. Results were FWE cluster-corrected (p < .05).*

Table S1. Results of the whole-brain repeated measures ANOVA for expected value.

Anatomical region	+/-	MNI coordinates x	y	z	T	*k*	*p*
Unique effect of risk							
R calcarine gyrus, including R superior occipital gyrus	+	15	-91	4	7,20	4446	< .001
R cuneus	+	18	-94	13	6,96		
R middle occipital gyrus, including L middle occipital gyrus, R lingual gyrus, R fusiform gyrus, L supramarginal gyrus	+	30	-91	10	6,95		
R postcentral gyrus	+	60	-19	52	5,90	631	< .001
R supramarginal gyrus, including R precentral gyrus, R superior frontal gyrus, R middle cingulate cortex	+	66	-28	40	5,81		
R caudate nucleus, including L caudate nucleus, L putamen	+	9	17	-5	5,19	295	< .001
R superior parietal lobe	+	27	-52	64	5,67	394	< .001
R precuneus	+	15	-58	61	5,14		
R paracentral lobe, including R inferior parietal lobe, R middle cingulate cortex	+	12	-31	52	4,06		
L inferior frontal gyrus (pars opercularis)	+	-57	8	7	4,59	97	.02
L temporal pole	+	-57	8	-2	3,98		
Unique effect of ambiguity							
R inferior parietal lobe	-	54	-37	52	4,48	88	.03
R middle temporal gyrus	-	69	-31	-2	4,12	89	.029
R middle temporal gyrus	-	60	-46	1	3,65		
R inferior frontal gyrus (pars triangularis)	-	54	23	28	3,95	143	.004
R inferior frontal gyrus (pars opercularis)	-	48	11	25	3,63		
R inferior frontal gyrus (pars triangularis), including R middle frontal gyrus	-	54	35	13	3,57		

Note: L = left; R = right. Anatomical labels are based on the Automated Anatomical Labeling (AAL) atlas. Results were FWE cluster-corrected (p < .05).